2016

High Temperature Oxidation of Indefinite Chill Roll Material Under Dry and Humid Atmospheres

Liang Hao
University of Wollongong, lh421@uowmail.edu.au

Zhengyi Jiang
University of Wollongong, jiang@uow.edu.au

Zhixin Chen
University of Wollongong, zchen@uow.edu.au

Dongbin Wei
University of Wollongong, dwei@uow.edu.au

Xiawei Cheng
University of Wollongong, xiawei@uow.edu.au

See next page for additional authors

High Temperature Oxidation of Indefinite Chill Roll Material Under Dry and Humid Atmospheres

Abstract

In this paper, the isothermal oxidation of the indefinite chill (IC) roll is investigated by using a thermogravimetric analyzer (TGA) from 550 to 700 °C under dry and humid atmospheres. It is found that the oxidation kinetics follow a linear trend and the oxide scale consists of two layers after the oxidation in dry air but three layers in humid air above 600 °C. In dry air, the graphite is covered by the oxide scale above 650 °C. The water vapor accelerates the oxidation of the matrix and the graphite. The graphite is covered by the extension of the oxide scale above 600 °C in humid air. The as-treated samples are examined with SEM and XRD, while the kinetics is based on TGA results.

Keywords

humid, dry, temperature, under, material, atmospheres, roll, high, chill, indefinite, oxidation

Disciplines

Engineering | Science and Technology Studies

Publication Details

Hao, L., Jiang, Z., Chen, Z., Wei, D., Cheng, X., Zhao, J., Luo, M., Ma, L., Luo, S. & Jiang, L. (2016). High Temperature Oxidation of Indefinite Chill Roll Material Under Dry and Humid Atmospheres. Steel Research International, 87 (3), 349-358.

Authors

Liang Hao, Zhengyi Jiang, Zhixin Chen, Dongbin Wei, Xiawei Cheng, Jingwei Zhao, Ming Luo, Li Ma, Suzhen Luo, and Laizhu Jiang

High temperature oxidation of indefinite chill roll material under dry and humid atmospheres

Liang Hao, Zhengyi Jiang*, Zhixin Chen, Dongbin Wei, Xiawei Cheng, Jingwei Zhao, Ming Luo, Li Ma, Suzhen Luo and Laizhu Jiang

ABSTRACT: In this paper, the isothermal oxidation of the indefinite chill (IC) roll was investigated by using a thermogravimetric analyser (TGA) from 550 to 700 ℃ under dry and humid atmospheres. It was found that the oxidation kinetics followed a linear trend, and the oxide scale consists of two layers after the oxidation in dry air but three layers in humid air above 600 ℃. In dry air, the graphite was covered by the oxide scale above 650 ℃. The water vapor accelerated the oxidation of the matrix and the graphite. The graphite was covered by the extension of the oxide scale above 600 ℃ in humid air. The as-treated samples were examined with SEM and XRD, while the kinetics was based on TGA results.
Keywords: IC roll, isothermal oxidation, thermogravimetric analyser (TGA)

1. Introduction

Hot rolled sheets and strips are primarily intermediate products that are used to produce cold rolled sheets and strips. Once the defects occurred in this process, it is very difficult to eliminate through the subsequent processes. Rolls with improved mechanical properties such as wear resistance, high strength, fracture toughness and thermal fatigue are essential for the quality improvement of rolled products and for roll durability [1-3]. Three types of roll materials are globally used, namely high chromium (Hi-Cr) steel, high speed steel (HSS) and indefinite chill (IC) roll materials. Hi-Cr steel, containing up to 18% chromium, has a good resistance to thermal oxidation. Nevertheless, sticking defects appeared in the last stages of hot rolling process, particular for ferritic stainless steels [4-10]. Studies have shown that the sticking problems are improved with the presence of oxide scales on the rolls. This is the reason why sticking worsens when Hi-Cr rolls are used, because with 18% Cr,

L. Hao, Prof. Z. Jiang*, Dr. Z. Chen, X. Cheng, Dr. J. Zhao
School of Mechanical, Materials and Mechatronic Engineering, University of Wollongong, NSW 2522, Australia
Dr. D. Wei
School of Electrical, Mechanical and Mechatronic Systems, University of Technology Sydney, NSW 2007, Australia
M. Luo, L. Ma, Dr. S. Luo, Dr L. Jiang
Baosteel Research Institute (R&D Centre), Baoshan Iron & Steel Co., Ltd., Shanghai 200431, PR China
Jiang@uow.edu.au

these steels are highly oxidation resistant. The further evolution was to reduce the amount of Cr to less 7% and add Mo, V, W and C to produce HSS. It has a higher strength but still difficult to be oxidised. IC roll materials, containing a substantial amount of graphite, have a good thermal and oxidation behaviour [11]. Because the graphite in the IC roll materials can retard crack propagation and reduce sticking as they lubricate the contact area between the roll and the rolled strips. It is reported that the sticking defects are obviously improved with the application of IC roll [12-16].

During the hot rolling, the surface temperature of work rolls can exceed 700℃ in a very short contact time (10^{-2} to 10^{-3} sec) because of the heat conducted from hot strips, deformation heat and friction heat, and then they are cooled to room temperature by spraying water for the rest of time in each cycle (2 to 10^{-1} sec) [17]. The total time of the work rolls in high temperature is less than 30 min in one period of roll changing, and oxide scale formed on the roll surface can be broken by friction and thermal fatigue. The purpose of this paper is to investigate the oxidation mechanism of IC roll material through a combined study of oxidation kinetics, and surface morphology and cross sections of the oxide scales formed by carrying out the isothermal oxidation in both dry and humid atmospheres at a temperature range from 550 to 700 ℃ up to 30 min. Oxidation kinetics and characteristics of oxide scale formed were systematically studied.

2. Experimental

The IC roll material studied was obtained directly from the shell part of a real work roll, and its chemical composition is listed in Table 1. Coupons with the dimensions of 15×10×1 mm^3 were machined and there is a 0.5 mm side length square hole near the top edge of the coupon. Two broad surfaces were polished up to 1 μm diamond and the rest surfaces were ground with 1200 grit sand paper. Then the samples were cleaned by means of ultrasonic agitation in ethanol and kept in vacuum desiccator before the tests.

Fe	C	Ni	Cr	Si	Mn	Mo
Balance	3.35	4.54	1.85	0.77	0.89	0.49

Table 1. Chemical compositions of the studied IC roll (wt. %)

The isothermal oxidation was investigated on a SETSYS Evolution S60/58507. SETSYS Evolution is equipped with a vertical hang down symmetrical balance and can work under corrosive and humid atmospheres. The SETSYS balance has the resolution down to 0.002 μg, and extremely low drifts and high precision over long periods of time. A WETSYS is used to provide a controlled humid atmosphere to simulate real hot rolling conditions. The controlled humid atmosphere is produced by passing dry air pass through a sealed water tank held at a given temperature. The maximum water temperature for WETSYS is 60 ℃ (corresponding to 20% water vapor in water-saturated gas), which is used in this investigation[18]. As a comparison, the oxidation behaviours of the IC are also investigated in dry air. The schematic diagram of the apparatus is illustrated in Figure 1. The isothermal oxidation experiments were conducted at the temperatures ranging from 550 to 700 ℃ for 30 min. The experimental details are given as follows: (a) the sample was suspended in the furnace which was then evacuated and filled with high purity Ar; (b) as the pressure of Ar reached 1 atm, the sample was heated to the testing temperatures at a rate of 25 ℃/min and held for 5 min once the testing temperature was reached. During the heating, Ar flowed through the furnace at a rate of 100 ml/min; (c) the oxidising gas was introduced at a rate of 100 ml/min, and the isothermal oxidation processed for 30 min; (d) the isothermal oxidation was terminated by replacing the oxidation gas with Ar to prevent further oxidation and the sample was cooled to room temperature at a rate of 99 ℃/min. The mass variations were recorded every 0.2 s in these processes.

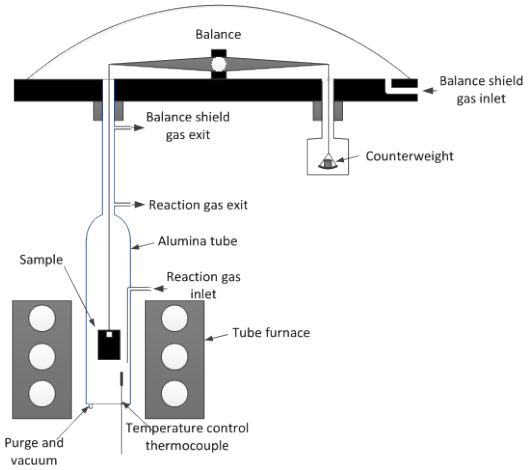

Figure 1. Schematic diagram of SETSYS Evolution S60/58507

Metallographic examination was carried out after the specimens were sectioned, ground, polished and etched with 2% Nital. An optical microscope (OM) was observed using a DM6000 optical microscope. Additionally, the morphology and the chemical composition of the oxidation products was determined with scanning electron microscopy (SEM) using a JEOL JSM 6490 and filled emission JEOL JSM-7001F SEM [19, 20]. The constitutions of the oxide scales were identified by X-ray diffraction (XRD) on a GBC MMA diffractometer. The cross-section segments have been cut from each sample, mounted in Bakelite, and polished down to 0.25 μm. the oxidation kinetics curves were obtained by plotting the mass change per surface area against the oxidation time.

3. Results

3.1. Microstructure of IC roll material

Figure 2a shows the optical micrograph of IC roll material etched by 2% Nital prior to the experiments. Three different phases, graphite, Fe_3C (cementite) and tempered martensite can be distinguished according to different contrasts and morphologies, in which coarse martensitic matrix mingles with a substantial amount of free graphite (dark region) and cementite (bright region) formed along the cell boundaries [21]. The graphite is reported to play a role in delaying the crack growth and in lubricating to prevent the rolled plates and the rolls from sticking [1]. The XRD spectrum (Figure 2b)

reveals two phases, cementite and iron matrix.

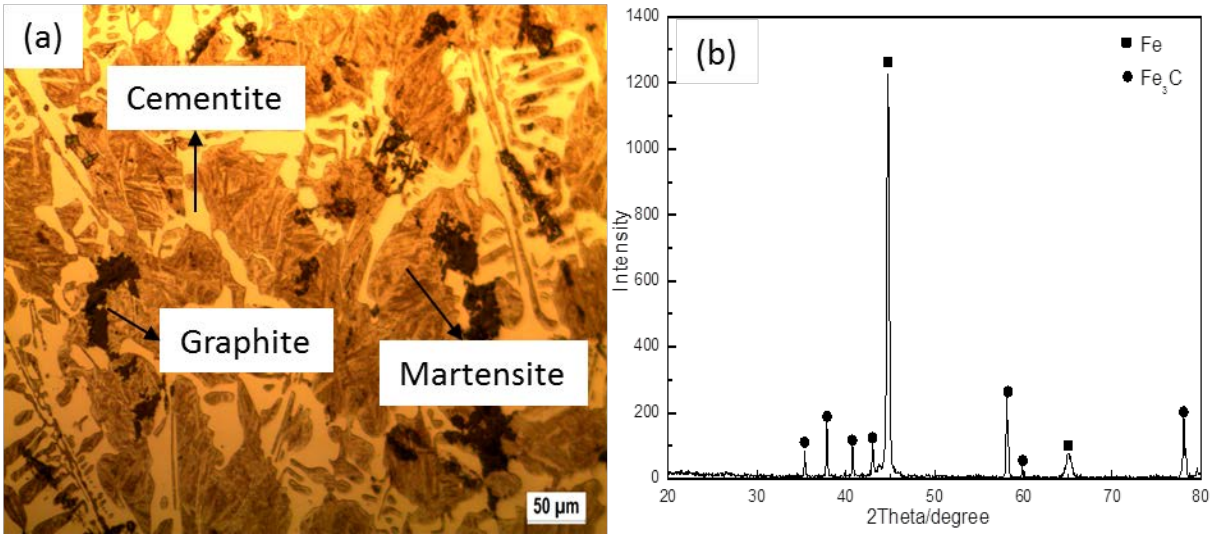

Figure 2. Optical micrograph (a) and XRD pattern of the studied IC roll (b).

3.2. Oxidation kinetics

The oxidation kinetics curves obtained under both dry and humid atmospheres are shown in Figure 3. It is observed that the influence of the temperature on the mass gain at different oxidising atmospheres varies, and its oxidation kinetics follows a roughly linear law. In dry air, the mass gain (Figure 3a), comparatively low at 550 ℃, rises gradually with the increase of the temperature until 650 ℃, and the oxidation rate at 700 ℃ demonstrates a lower mass gain than that at 650 ℃, even lower than that at 600 ℃ at later stage. However, the presence of water vapor in the atmosphere accelerates the mass gain of the sample at each temperature. In addition to that, the mass gain (Figure 3b), reveals a linear trend and obviously goes up with the increase of the oxidation temperature.

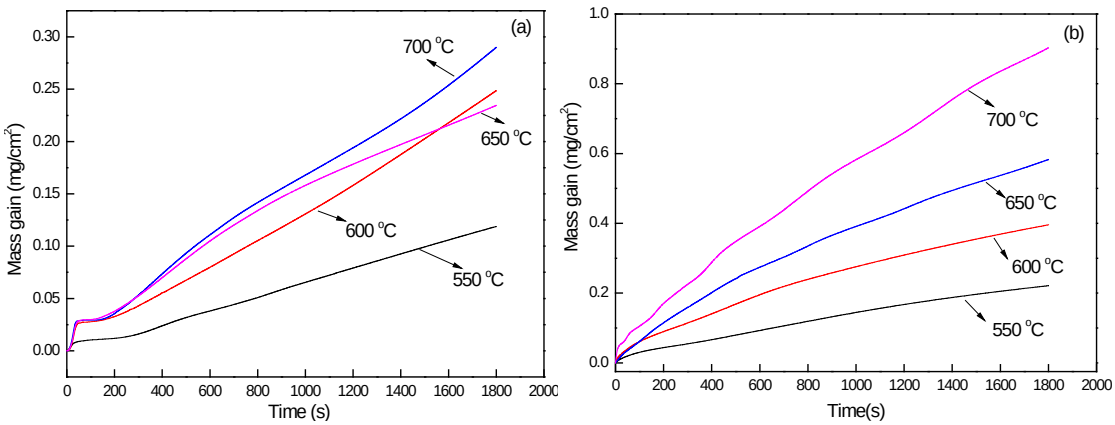

Figure 3. Isothermal oxidation curves of IC samples at different temperatures in dry (a) and humid atmospheres (b)

3.3. Surface morphologies analysis

3.3.1. Oxidise in dry air

Figure 4 shows SEM images of the samples oxidised at the different temperatures for 30 min in dry air. Different surface morphologies can be seen after the oxidation at different temperatures. At 550 ℃ (Figure 4a), the surface morphology was comparatively flat, and the shallow grooves were only located at the grain boundaries. The grooves were deepening at 600 ℃ (Figure 4b). It is because the oxide scales grown on the matrix protruded out while the cementite at the grain boundaries was slowly oxidised, thus the grain boundaries seem to be sunken. The selection oxidation takes place at these temperatures due to that different alloy compositions and microstructures between the matrix and the cementite. As the oxidation processed at 650 ℃ (Figure 4c), the oxidation of the cementite at grain boundaries became obvious, which makes the grooves to be shallower. At 700 ℃, the oxide scales covered the whole surface with the invisibility of initial grain boundaries and tended to peel off (circled area in Figure 4d).

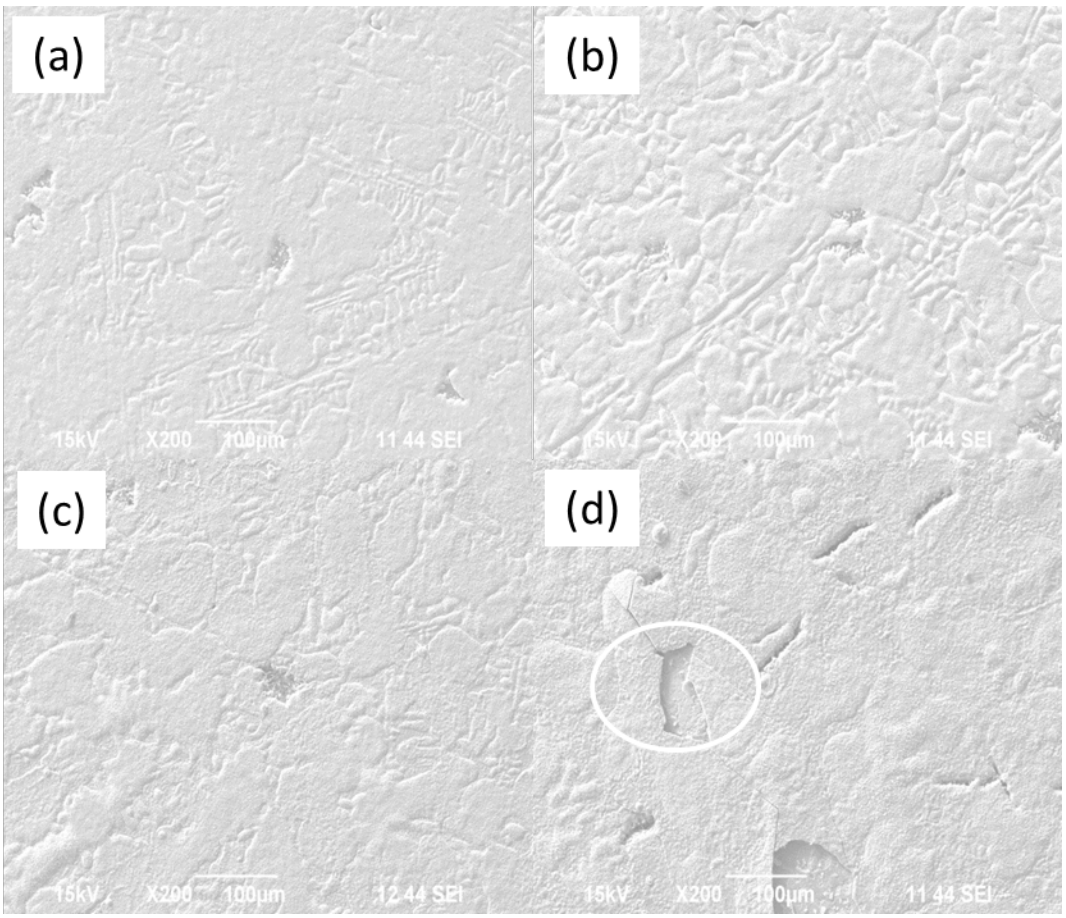

Figure 4. SEM images of the samples oxidised at the temperatures in dry air: (a) 550 ℃, (b) 600 ℃, (c) 650 ℃ and (d) 700 ℃.

3.3.2. Oxidise in humid air

Figure 5 shows SEM images of the samples oxidised at the temperatures between 550 and 700 ℃ in humid air. The morphologies of the surfaces were significantly different from those oxidised in dry air. Although the presence of water vapor, the sample was gently oxidised and present similar pattern as the sample oxidised in dry air at 550 ℃ (Figure 4a). The surface morphology, however, was more homogeneous at 600 ℃ in humid air (Figure 5b) than that of in dry air, with the disappearing of the grain boundaries. Because the oxidation of the Fe_3C (cementite) accelerated in humid air at this temperature. At 650 and 700 ℃, the surfaces (Figures 5c and d) were more uneven than their counterparts in dry air (Figures 4c and d). The water vapor intensified the oxidation rate at the higher temperatures, and the oxide scales formed in humid air adhered firmly to the matrix unlike the oxide scales produced in dry air which tended to peel off.

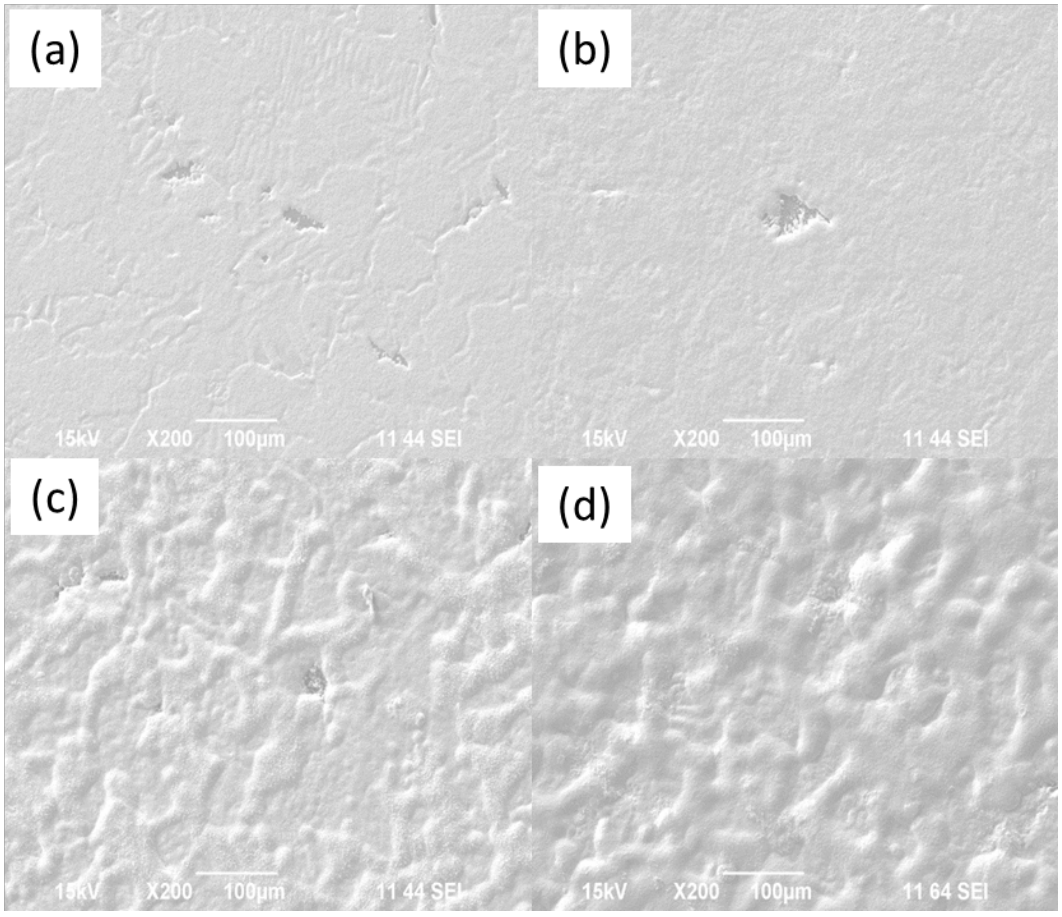

Figure 5. SEM images of the samples oxidised at the temperatures in humid air: (a) 550 ℃, (b) 600 ℃, (c) 650 ℃ and (d) 700 ℃.

3.4. X-ray structural analysis

Figure 6 shows XRD patterns of the IC samples after the oxidation at the different temperatures in both dry and humid atmospheres. In dry air, iron and cementite phases are revealed at all temperatures, indicating that the thickness of the oxide scales is less than the depth of X-ray diffraction. As the increase of the testing temperature, the main phases are transformed to hematite (Fe_2O_3) and magnetite (Fe_3O_4) at the high temperature, showing the oxidation is getting more severe and the thin oxide scale is penetrated by XRD ray. Comparing with the oxidation products obtained in dry air, the intensity of hematite and magnetite is higher but lower for iron and cementite at 550 and 600 ℃, and only iron oxides are revealed at high temperature, indicating that the thick oxide scale and the fact that the ray of XRD cannot penetrate deeply to detect the matrix phase.

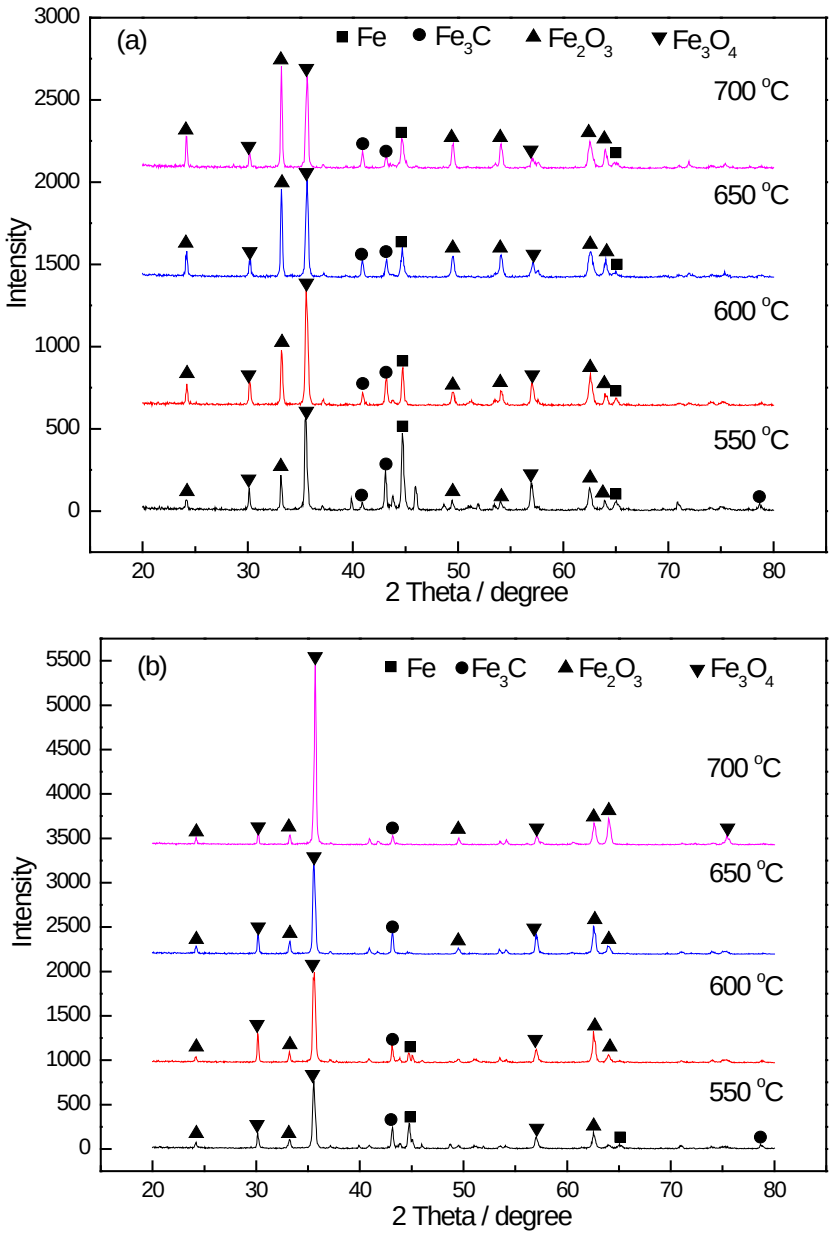

Figure 6. XRD patterns of the IC samples after the oxidation at different temperatures in dry (a) and humid atmospheres (b).

4. Discussion

For the quantitative estimation of the performance of the IC roll material in an oxidising environment, a mathematic model is necessary. For this purpose, the most efficient way is to consider the mass gain Δm as a function of the exposure time t in the oxidising atmosphere, while the rest of factors influencing oxidation are expressed by a oxidation rate constant K_p. Hence, the comparison of the performance is reduced to the determination of the function that binds Δm and t

along with the calculation of the constant K_p [22].

Instead of a parabolic rate law used for a limited number of metals at stable states, oxidation kinetics of the IC material approximately obey a linear trend. Therefore, a linear rate law is expressed to fit the oxidation kinetics data below:

$$\Delta m = K_p t \quad (1)$$

where Δm is the weight gain per unit area. t is the oxidation time and K_p is the oxidation rate constant.

According to Arrhenius equation, the oxidation rate constant was found to be an exponential function of temperature:

$$K_p = K_0 \exp(\frac{-E}{RT}) \quad (2)$$

where K_o is the pre-exponential factor, E is the apparent activation energy, R is the gas constant and T is the absolute temperature. The curves of the natural logarithm of kp vs 1000/T under two oxidising conditions are shown in Figure 7, from which can be obtained that he activation energy E are 28.443 and 55.28 kJ/mol for dry and humid atmospheres, respectively, and the R-squared (R^2) has a higher accuracy in humid atmosphere (0.99) than that in dry atmosphere (0.81). Therefore, the oxidation kinetics is better fit in linear law for humid air than in dry air.

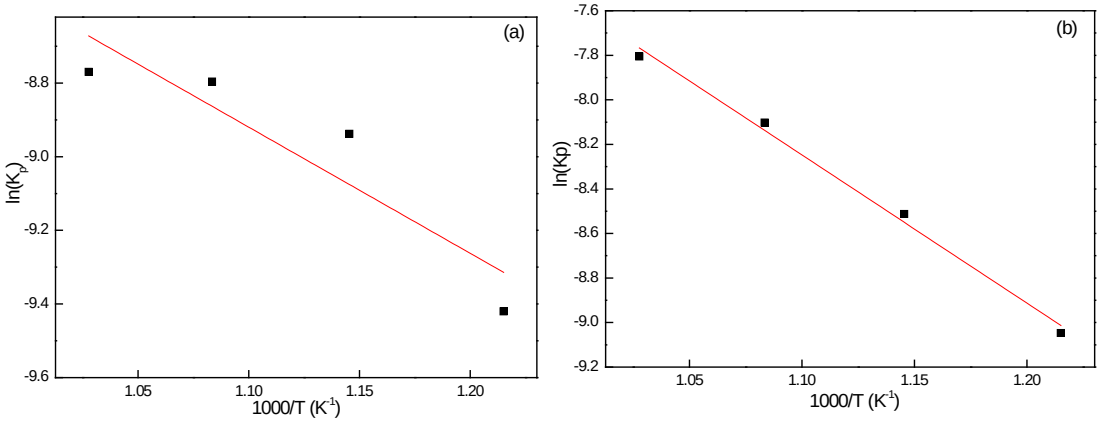

Figure 7. Dependence of the oxidation rate constant with temperature in dry (a) and humid atmospheres (b)

Figure 8 shows cross sections and the correspondent EDS line scanning analysis of the IC oxidised in dry air. The oxide scale consists of two distinctive layers. The EDS

line scanning analysis show that the thin layer located at next to the substrate is Cr-rich, it is believed to be $(FeCr)_3O_4$, and the thick oxide layer at the scale-gas interface containing only iron and oxygen is thought to be hematite (Fe_2O_3). The intensity of Si at the metal-oxide scale interface reveals no obvious difference between the substrate and the oxide scale at 550 ℃, but a higher intensity of Si was observed in the substrate beneath the oxide scale than in the oxide scale at 600 and 650 ℃. The similar phenomenon was also observed for the intensity of Ni, namely, the intensity of Ni beneath the oxide layer increases gradually as the increase of the temperature.

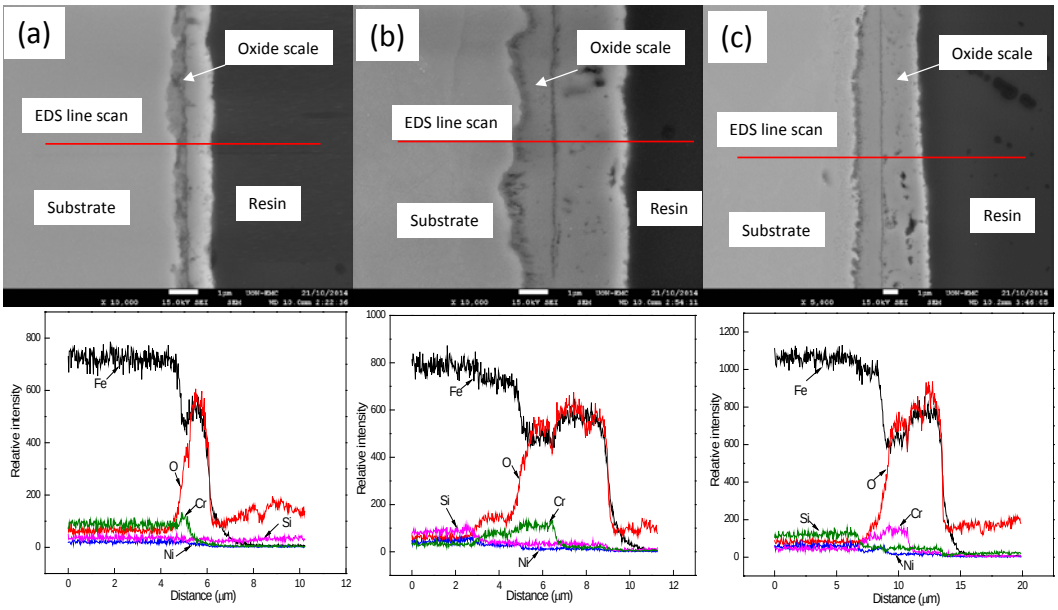

Figure 8. Cross sections and EDS line scanning element analysis of the IC oxidised in dry air for 30 min: (a) 550 ℃, (b) 600 ℃ and (c) 650 ℃.

Figure 9 shows SEM X-ray maps of the cross section of the IC oxidisied at 700 ℃ for 30 min in dry air, from which two oxide layers can be seen, a thin Cr-rich layer next to the substrate and a thick Fe-O-rich layer. Neither Si or Ni is present in the oxide scale, which indicates that it can hardly diffuse into the oxide scale at 700 ℃ in dry air.

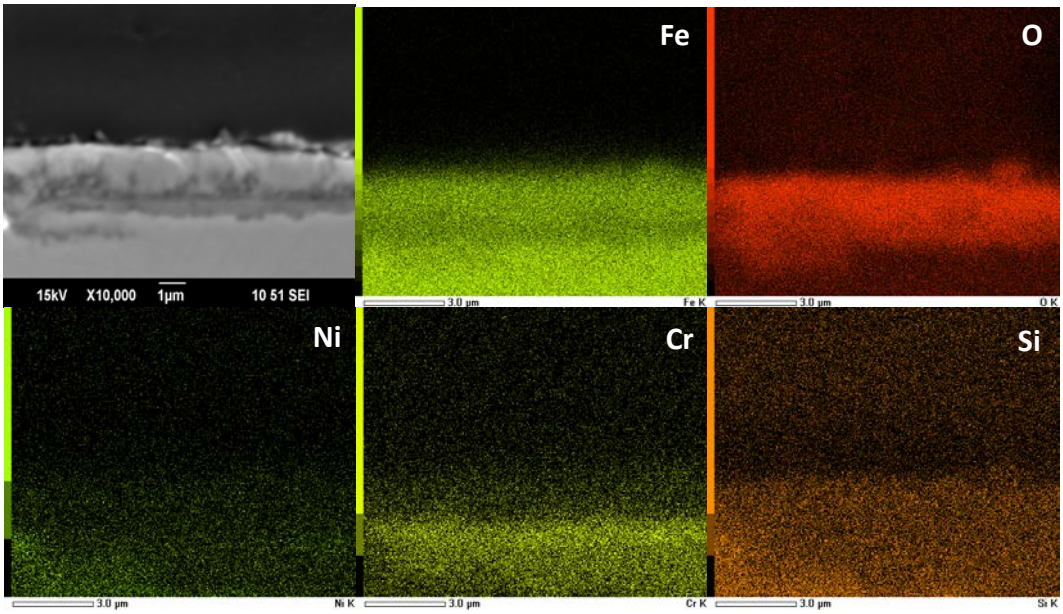

Figure 9. SEM X-ray maps for the IC oxidised at 700 ℃ for 30min in dry air

Figure 10 shows cross sections and the correspondent EDS line scanning analysis of the IC oxidised in humid air. The morphologies of the cross sections of the oxide scale are quite different from that of in dry air. At 550℃, two distinctive oxide layers were observed and the EDS line scanning analysis show that the thin layer located at next to the substrate is Cr-rich $(FeCr)_3O_4$, and the thick outer oxide layer containing only iron and oxygen is thought to be hematite (Fe_2O_3). As the oxidising temperatures reach 600 and 650℃, however, the oxide scale was comprised of three oxide species, namely an Cr-rich layer next to the substrate, a thick middle layer of magnetite (Fe_3O_4) and a thin outer layer of hematite (Fe_2O_3) at oxide-gas interface. Moreover, the intensities of Si and Ni are higher in the substrate beneath the oxide scale than that in the oxide scale at the three temperatures, indicating that Si and Ni rarely diffuse into the oxide layers.

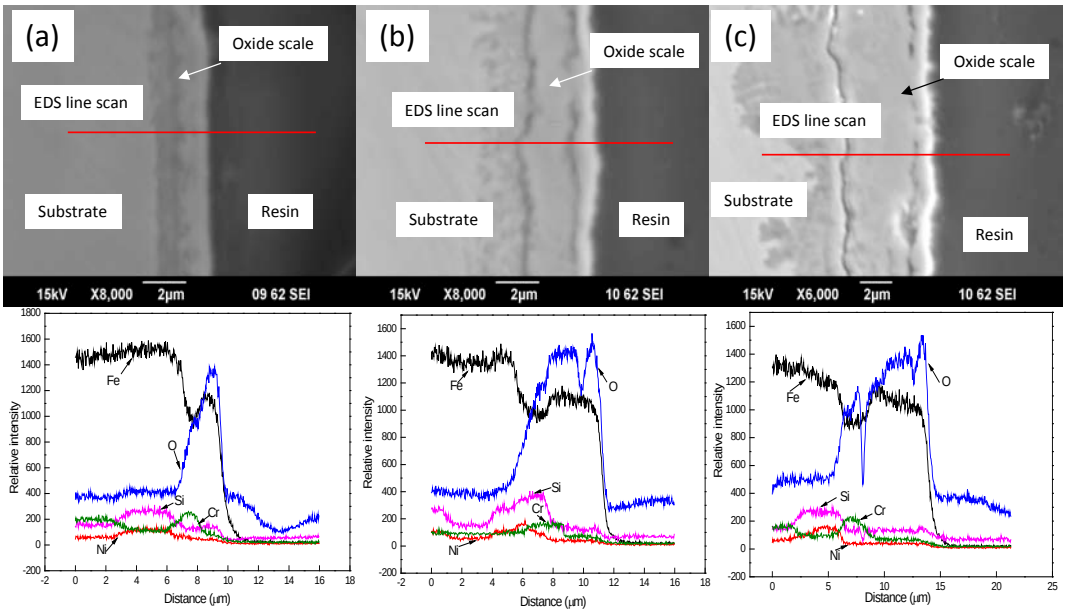

Figure 10. Cross sections and EDS line scanning element analysis of the IC oxidised in humid air for 30 min: (a) 550 ℃, (b) 600 ℃ and (c) 650 ℃.

Figure 11 shows SEM X-ray maps for the IC oxidised at 700 ℃ in humid air. Three oxide phases were also observed. Both Si and Ni are only present in the substrate beneath the inner oxide, revealing that Si and Ni can hardly diffuse into the oxide scales; whereas Cr intensifies in the inner oxide, showing that the inner oxidation results in consuming Cr element.

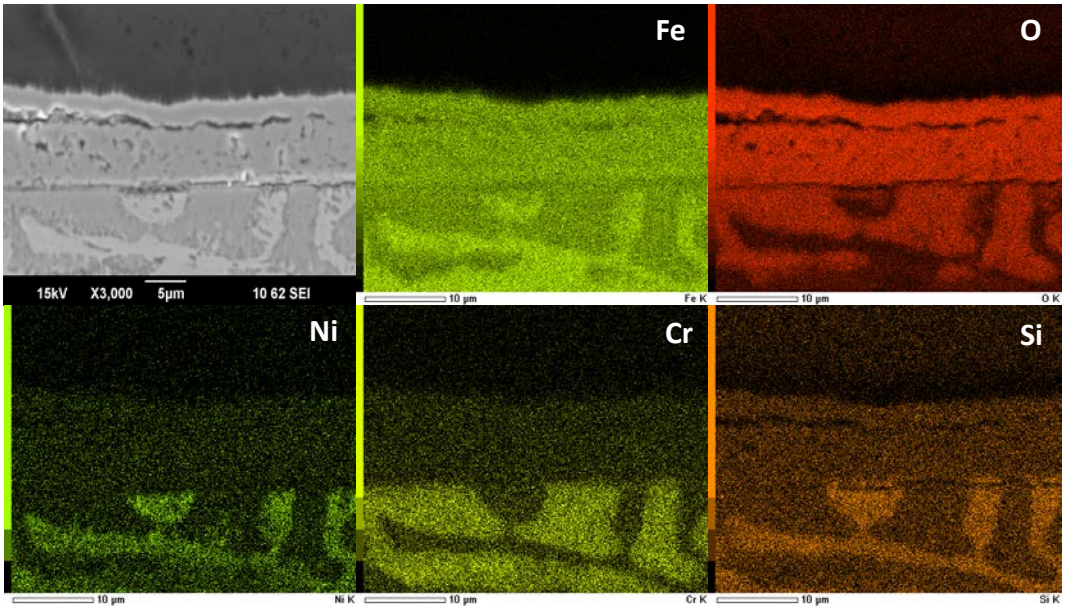

Figure 11. SEM X-ray maps for the IC oxidised at 700 ℃ for 30min in humid air

A significant feature of the IC roll materials is the presence of a substantial amount of free graphite, which greatly improves the ability of the roll to withstand the thermal

shocks associated with hot rolling steel strip, and greatly reduces the potential for fusing of the strip to the roll [23]. Therefore, the degradation of graphite due to oxidation directly affected its functionality. Figure 12 shows cross sectional images of the graphites after the oxidation in dry air. It can be seen that the morphologies of the graphites exhibit different characteristics after the oxidation in different temperatures. The oxidation of graphite known as decarburisation denudes the graphite connected to the surface and leaves empty cavities [24]. After the oxidation at 550 and 600 ℃, the graphite surface sinks due to the fact that the oxidation of the graphite results in the loss of the graphite, but the graphite still exposes outside. At 650 ℃, the loss of the graphite and the growth of the oxide scale lead to the graphite totally covered by the oxide scale. After the further oxidation at 700 ℃, the oxide scale covered on the graphite grows thicker, and tends to fill the cavities caused by the oxidation the graphite.

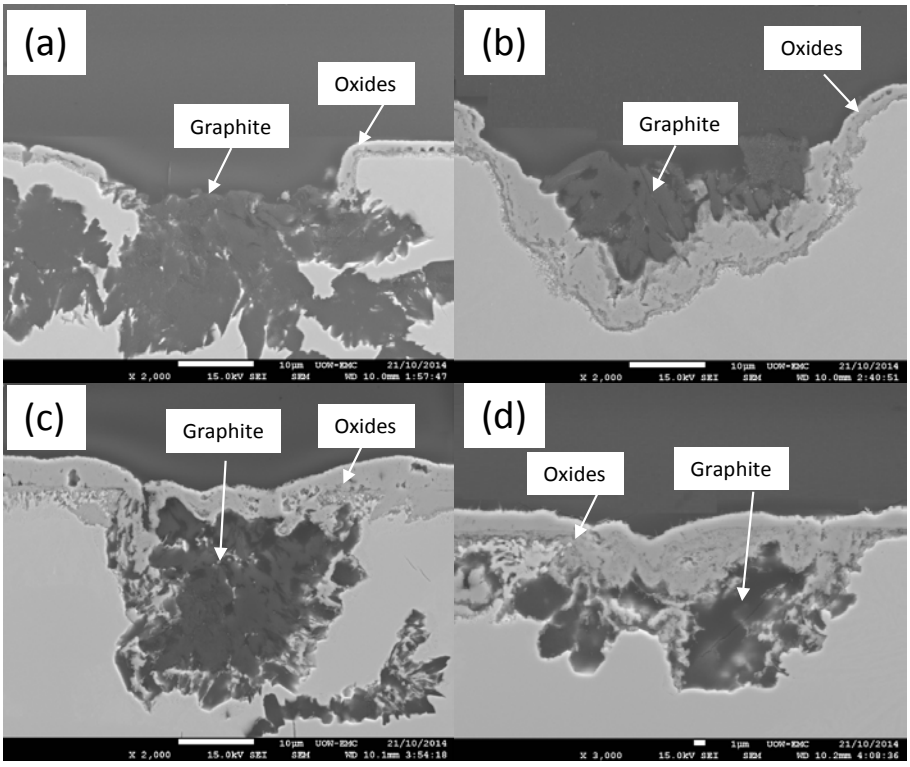

Figure 12. Cross sectional images of the graphites after the oxidation in dry air for 30 min: (a) 550 ℃, (b) 600 ℃, (c) 650 ℃, and (d) 700 ℃.

Figure 13 shows cross sectional images of the graphites after the oxidation in humid air. The morphologies of the graphites after the oxidation in humid air are different

from those in dry air. The water vapor accelerates the growth of the oxide scale and the loss of the graphite. The graphite, still exposes outside after the oxidation at 550 ℃, is covered by the oxide scale at 600 ℃. At 650 ℃, the oxide scale extends to fill the graphite cavities. After the oxidation at 700 ℃, the graphite is nearly completely consumed and filled by the extension of the oxide scale, which makes the graphite ineffective to play its role in hot rolling.

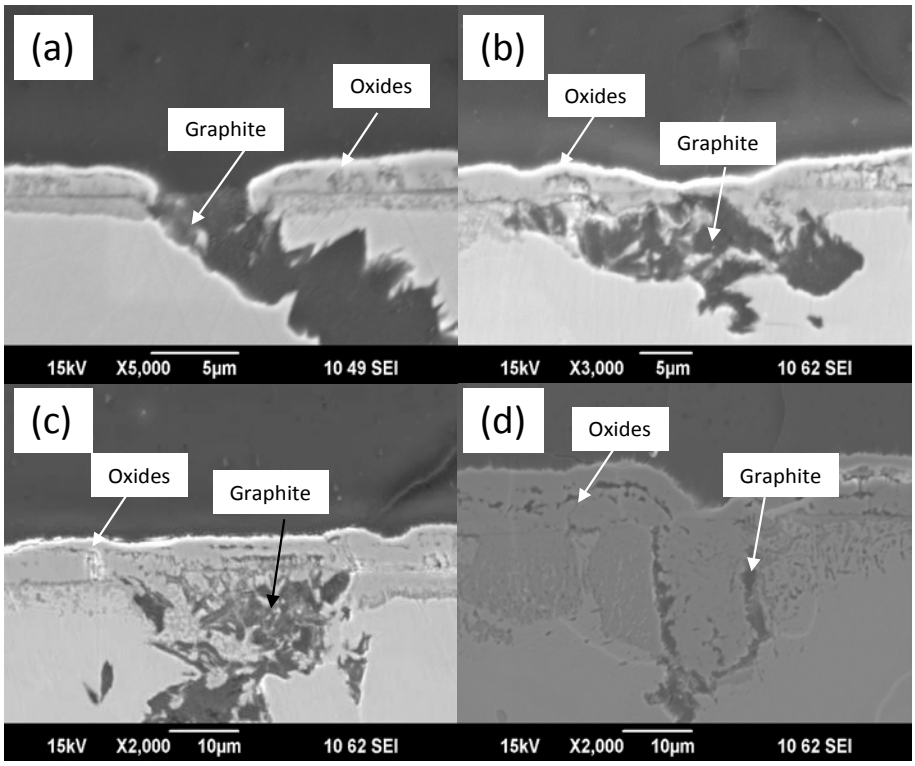

Figure 13. Cross sectional images of the graphites after the oxidation in humid air for 30 min: (a) 550 ℃, (b) 600 ℃, (c) 650 ℃, and (d) 700 ℃.

5. Conclusions

The isothermal oxidation investigation of the IC material was investigated on a TGA at the temperatures from 550 to 700 ℃ for 30 min under dry and humid atmospheres. The following conclusions can be obtained:

1. In dry air, the oxidation kinetics of the IC samples show that the mass gain, revealing a linear trend, rises gradually with the increase of the temperature until 650 ℃, and the oxidation rate at 700 ℃ is lower than that at 650 ℃. In humid air, however, the mass gain shows a linear trend and obviously goes up

with the increase of the oxidation temperature.

2. The oxide scale of the IC after oxidation in dry air is made up of two oxide layers: an inner thin Cr-rich layer ($(FeCr)_3O_4$) next to the substrate and an outer thick layer of hematite at the metal-gas interface. Above 600 ℃, the oxide scale of the IC oxidised in humid air consists of three oxide species: an inner Cr-rich layer next to the substrate, a middle layer of magnetite and an outer layer of hematite. Si and Ni rarely diffuse into the oxide layers.
3. In humid air, the graphite was consumed and covered by the extension of the oxide scale above 600 ℃. The roll temperature of the IC should be controlled below 600 ℃ in order to be effectively applied in the hot rolling mill.

Acknowledgments

The authors acknowledge the Baosteel - Australia Joint Centre financial support for current project, and UOW Electron Microscopy Centre (EMC) for the equipment provided.

References

[1] S. Lee, D. Kim, J. Ryu and K. Shin, Metallurgical and Materials Transactions A. 1997, 28, 2595.
[2] J.-W. Choi and D. Kim, ISIJ International. 1999, 39, 823.
[3] P. Pathak, S. Jha and A. Singh, International Journal of Technical Research. 2012, 1,
[4] W. Jin, J.-Y. Choi and Y.-Y. Lee, ISIJ International. 1998, 38, 739.
[5] W. Jin, J. Y. Choi and Y. Y. Lee, Isij International. 2000, 40, 789.
[6] Jong Seog Lee, Chang-Young Son, Chang Kyu Kim and D. J. Ha, Advanced Materials Research. 2007, 26-28,
[7] J. S. Lee, C. Y. Son, C. K. Kim, D. J. Ha, K. T. Kim and Y. D. Lee, Advanced Materials and Processing. 2007, 26-28, 3.
[8] J. X. Liu, Y. J. Zhang and J. T. Han, International Journal of Minerals, Metallurgy, and Materials. 2010, 17, 573.
[9] C. Y. Son, C. K. Kim, D. J. Ha, S. Lee, J. S. Lee, K. T. Kim and Y. D. Lee, MetallURGICAL AND MATERIALS TRANSACTIONS A. 2007, 38, 2776.
[10] T. Toriumi and A. Azushima, Tetsu to Hagane-Journal of the Iron and Steel Institute of Japan. 2011, 97, 388.
[11] F. J. Pérez, L. Martínez, M. P. Hierro, C. Gómez, A. L. Portela, G. N. Pucci, D. Duday, J. Lecomte-Beckers and Y. Greday, Corrosion Science. 2006, 48, 472.
[12] D. J. Ha, Y. Jin., J. S. Lee and S. Lee, Metallurgical and Materials Transactions A.

2009, 40, 1080.
[13] D. J. Ha, C.-Y. Son, J. W. Park, J. S. Lee, Y. D. Lee and S. Lee, Materials Science and Engineering. 2008, A 492, 49.
[14] D. J. Ha, H. K. Sung, S. Lee, J. S. Lee and Y. D. Lee, Materials Science and Engineering: A. 2009, 507, 66.
[15] M. Andersson, R. Finnström and T. Nylén, Ironmaking & Steelmaking. 2004, 31, 383.
[16] J. H. Beynon, Tribology International. 1998, 31, 73.
[17] O. Kato, H. Yamamoto, M. Ataka and K. Nakajima, ISIJ International. 1992, 32, 1216.
[18] J.-Y. Yun, S.-A. Ha, C.-Y. Kang and J.-P. Wang, Steel research international. 2013, 84, 1252.
[19] M. Norden, G. Paul, M. Blumenau, T. Heller and K. J. Peters, Steel research international. 2011, 82, 839.
[20] L. Cho and B. C. De Cooman, Steel research international. 2012, 83, 391.
[21] G. Byun, S. Oh, C. Lee and S. Lee, Metallurgical and Materials Transactions A. 1999, 30, 234.
[22] G. Vourlias, N. Pistofidis and K. Chrissafis, Thermochimica Acta. 2008, 478, 28.
[23] B. T. K. Nylen and T. P. Adams, US6013141, 1997.
[24] S. Ghodrat, M. Janssen, L. I. Kestens and J. Sietsma, Oxidation of Metals. 2013, 80, 161.